Dentistry
ISSN: 2161-1122

Rashid, et al., Dentistry 2019, 9:3
DOI: 10.4172/2161-1122.1000539

Research Article Open Access

Valproic Acid Contributes to Bone Cavity Healing in Rats

Mamunur Rashid, Yosuke Akiba*, Kaori Eguchi, Nami Akiba, Masaru Kaku, Masako Nagasawa and Katsumi Uoshima

Division of Bio-prosthodontics, Department of Oral Health Science, Niigata University Graduate School of Medical and Dental Sciences, Niigata, Japan

***Corresponding author:** Dr. Yosuke Akiba, Department of Oral Health Science, Niigata University Graduate School of Medical and Dental Sciences, 2-5274 Gakkocho-dori, Chuo-ku, Niigata, 951-8514, Japan, Tel: +81-25-227-2900; Fax: +81-25-227-2899; E-mail: yoakiba@dent.niigata-u.ac.jp

Received date: March 25, 2019; **Accepted date:** April 03, 2019; **Published date:** April 10, 2019

Abstract

Background: Sufficient bone quality and quantity are necessary for successful results in a dental implant. Although numerous bone augmentation methods have been reported, used in the clinic and showed successful results in some extent, more reliable methods are still required. Valproic Acid (VPA) which was known as an Anti-epilepsy agent and histone deacetylases inhibitor regulate osteoblast differentiation through Runx2 activation *in vitro*. The present study aimed to evaluate the effects of systemic administration of VPA on bone regeneration in rat maxillary bone cavity.

Material and Methods: Fifty-four Wistar rats were used for the experiment. Upper first and second molars were extracted at 4 weeks. Three weeks after extraction, the experimental group received intraperitoneal (IP) injection of VPA and control group received IP injection of saline for 7 days prior to the preparation of bone cavity at the first molar area. Rats were sacrificed on days 3, 7, 14, and 21, and samples were prepared for micro-CT and histological analyses and serum Alkaline Phosphatase (ALP) activity was measured. After 7 days of VPA or saline injection, bone marrow-derived cells were corrected for microarray analysis.

Results: Micro-CT analysis and histological observations confirmed higher amounts of newly formed bone, bone volume fraction (BV/TV) and trabecular thickness (Tb.Th), and less trabecular separation (Tb.Sp) in the experimental group at 7, 14, and 21 days than the control. VPA-treated animals showed significantly higher ALP activities at 7, 14, and 21 days than the control. From microarray analysis, 26 genes showed significantly altered expression.

Conclusion: As systemic administration of VPA accelerated bone regeneration in the rat maxillary bone cavity, there the possibility that VPA injection may be useful for bone augmentation therapy.

Keywords: Bone regeneration; Histone deacetylase inhibitors (HDACi); Valproic acid (VPA); Bone cavity

Introduction

The concepts of 'top-down treatment' and 'prosthetic driven implants' are essential for appropriate replacement of the lost teeth with dental implants. In this regard, sufficient bone quality and quantity to support implants are prerequisites. Loss of teeth often results in complex horizontal and vertical alveolar ridge defects. Therefore, alveolar bone augmentation before placement of dental implants is often required. Various bone augmentation techniques using autogenous bone grafts alone or combined with bone substitutes have been achieving a certain degree of success. They possess osteogenic, osteoconductive, and osteoinductive properties [1,2]. However, although autologous bone grafts exhibit high variability in their osteogenic potential among harvest sites and individuals [3], they could result in a less than desirable clinical outcome. In addition, they have limitations mainly because of donor site morbidity, infection, and/or delayed healing [4-7]. Bone substitutes mostly used as hydroxyapatite or β-tricalcium phosphate matrices have been shown to be osteoconductive [5,8]. However, no reliable long-term alternatives to autogenous bone grafts have been established to date [9]. Growth-factor-based regenerative therapies and/or multipotent ex vivo expanded cells for tissue engineering have yet to be realized with satisfying and predictable outcomes [10-12]. Although numerous bone augmentation methods have been reported, used in the clinic and showed successful results in some extent, some clinical problems have been left such as engraftment of transplanted bone, limitation of augmented bone volume or resorption of augmented bone. Therefore, improved and more reliable procedures for bone regeneration are necessary to optimize treatment outcomes. Epigenetic regulation of gene expression is recognized as a central mechanism that governs cell stemness, determination, commitment, and differentiation [13-17]. Histone Acetyl-Transferases (HATs) and Histone Deacetylases (HDACs) are enzymes involved in the remodeling of chromatin structure and epigenetic integrity. HATs are responsible for acetylation of histone, which promotes a more relaxed chromatin structure, allowing transcriptional activation. On the other hand, HDACs promote chromatin condensation and acts as a transcription repressor [18]. Eighteen HDACs have been identified in humans, and they are divided into four subclasses: class I HDACs (1, 2, 3, and 8), class IIa HDACs (4, 5, 7, and 9), class IIb HDACs (6 and 10), class III HDACs (SIRT1 to 7), and class IV HDACs (HDAC11). Runx2 activity has been implicated in the inhibitory action of HDACs in osteoblast differentiation. Several Class I HDACs (HDAC1 and 3) and class II HDACs (HDAC4, 5, 6 and 7) interact with Runx2 and repress its transcriptional activity [19-22]. Histone deacetylase inhibitors (HDACi) regulate osteoblast differentiation by enhancing Runx2-dependent transcriptional activation and accelerate osteogenesis

through up-regulating osteoblast marker genes in Mesenchymal Stem Cells (MSCs) of bone marrow [23], osteogenic cell lines [24], and murine calvarial organ cultures [25]. Valproic acid (2-n-propylpentanoic acid, VPA) is an effective antiepileptic drug that has been used for more than 30 years. VPA contribute to antiepileptic effect through inhibiting GABA degradative enzymes, such as GABA transaminase, succinate-semialdehyde dehydrogenase and by inhibiting the re-uptake of GABA by neuronal cells. Under dosage control conditions, VPA thought to be safe and effective. However, long term and high dose application, VPA showed adverse effects such as nausea, drowsiness, dizziness or vomiting or cause premature growth plate ossification in children and adolescents, resulting in decreased height [23]. The HDACi activity of VPA has been investigated [26,27], and it was confirmed to suppress class I and class II HDACs. VPA promotes cell proliferation of the pre-osteoblast cell line and activates Runx2 transcriptional activity in MC3T3-E1 [24]. VPA induced differentiation and accelerated mineralization of human mesenchymal stem cells [23] and pulp-derived cells [28]. Although previous *in vitro* studies have confirmed the beneficial effects of VPA on osteoblast differentiation and mineralization, it remains unknown whether systemic administration of VPA is able to improve bone regeneration *in vivo*. The objective of this study was to evaluate the effects of systemically administrated VPA on bone healing of maxillary bone defect in rats. In this study, bone cavity healing was assessed and the results will be applied to establishing a novel bone augmentation therapy using epigenetic theory.

Materials and Methods

Animals and experimental procedure

Fifty-four 4-week-old male Wistar rats (Charles River, Yokohama, Japan) were divided into control and experimental groups. At the age of 4 weeks, under anesthesia by an intraperitoneal injection of 8% chloral hydrate (400 mg/kg), 1st and 2nd maxillary molars on both sides were extracted. At 3 weeks after extraction, the experimental group received intraperitoneal (IP) injection of VPA at a dose of 300 mg/kg twice daily [29] and the control group received a saline injection for 7 consecutive days before cavity preparation. Body weight of all rats (both experimental and control groups) was measured once a day for consecutive 7 days during the period of VPA and saline injection.At the age of 8 weeks, under the same anesthesia, full-thickness flaps were elevated at recipient sites (the maxillary 1st molar area on both sides) and bone cavities were prepared by drilling with a slow speed dental handpiece at 500 rpm equipped with a Peeso-reamer (diameter 1.7 mm) in both groups. Profuse irrigation with sterilized physiological saline was maintained throughout drilling. Flaps were repositioned and sutured with nylon. All animal experiments in this study were approved by the Ethics Committee of Niigata University and were conducted in accordance with the Niigata University Guidelines for Animal Experimentation.

Micro-CT images and bone analysis

In the present study, samples at 7, 14 and 21 days were scanned in the same manner using a micro-CT scanner (Elescan, Tokyo, Japan). Briefly, the maxilla was placed on a custom made jig with axial direction and palatal area facing towards scanner. Scanning was performed at 53 kV, 100 μA and 900 projections, with a 0.5-mm aluminum filter. Based on the serial scanned images, 3D images were reconstructed using TRI/3D-BON software (RATOC, Tokyo, Japan). As the main purpose was to observe and analyze newly formed bone, the Region Of Interest (ROI) was selected in the area of the bone defect (Figure 1). Bone volume fraction (BV/TV), trabecular thickness (Tb.Th), and trabecular separation (Tb.Sp) within the ROI, which represent the percentage of mineralized bone volume in a given volume of total bone tissue within the bone cavity, and the thickness and organization of trabeculae, respectively, were calculated.

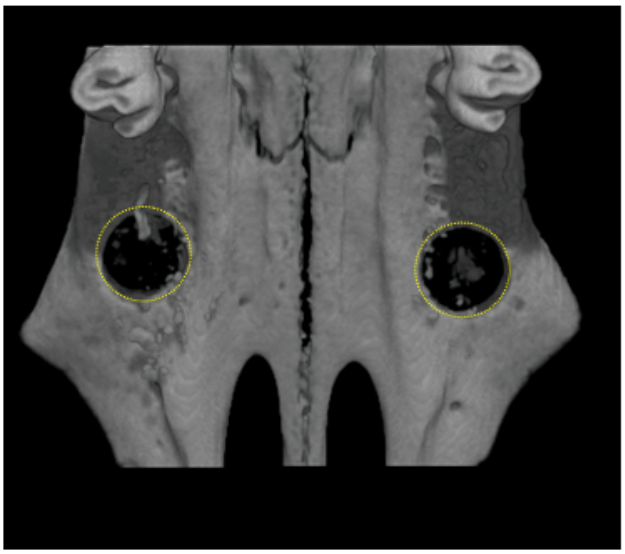

Figure 1: Three-dimensional construct of micro-CT image of rat maxilla showing third molars and bone cavities. Bone cavities which diameter 1.7 mm were prepared at the upper first molar areas on both sides at 4 weeks after extraction. Regions of interest (ROI) are shown in yellow circles.

Serum alkaline phosphatase (ALP) activity measurement

Blood samples were collected during euthanasia at 3, 7, 14, and 21 days after cavity preparation. Blood was allowed to clot and was centrifuged at 3000 rpm for 10 min [30]. Serum was harvested and stored at −20°C until biochemical assays. ALP activity was measured using an ALP kit (Takara, Shiga, Japan). Briefly, serum samples were diluted with extraction solution in accordance with the manufacturer's instructions. Initially, 50 μl of diluted serum from each sample was taken in each well of a 96-well plate. Then, 50 μl of substrate solution was added and the plate was maintained at 37°C for 60 min. Subsequently, 50 μl of stop solution (0.5 N NaOH) was added to each well. Absorbance was measured at 405 nm using a microplate reader. Each experimental sample was assayed in triplicate.

Histological Observation

Animals were sacrificed at 3, 7, 14, and 21 days after cavity formation. At the appointed times, they were anesthetized and fixed with transcardiac perfusion with a fixative containing 4% paraformaldehyde (pH 7.4). Specimens were decalcified in 10% EDTA solution for 4 weeks at 4°C. Serial paraffin sections were prepared sagittally at 5-μm thickness, and sections from the most central part of the defect were selected and stained with hematoxylin and eosin for histological observation.

Microarray analysis

Seven days after VPA or Saline injection, adherent cells from bone marrow were collected. Total cellular RNAs were extracted using RNeasy mini kit (Qiagen, Inc., Valencia, CA, USA). Microarray analysis was performed by Filgen, inc., using Array-readyOligo set rat version 3.0 arrays (Qiagen) which contain 31,769 long-mer probes representing 24,878 genes and 32,829 gene transcripts, a GenePix 4000B scanner (Axon Instruments, Union City, CA, USA), and Array-Pro Analyzer 4.5 software (MediaCybernetics, Inc., Bethesda, MD, USA). The RNA quality was assessed by Filgen (Filgen, Inc., Aichi, Japan) prior to the microarray analysis.

Statistical analysis

All numerical data are indicated as means ± SD (n>3). Two-group comparisons were performed using the non-parametric Kruskal-Walls test. Statistical significance was defined at $p<0.05$.

Results

Body weight

Both control group (n=27) and experimental group (n=27) showed a slight increase of body weight (from control at day 1, 338.5 ± 14.0119 to control day 7, 366.25 ± 14.0327 vs VPA at day 1, 337.75 ± 19.1557 to VPA at day 7, 357 ± 16.4797). No significant differences in body weight were observed between the control and experimental group during the period of saline and VPA injection (Figure 2).

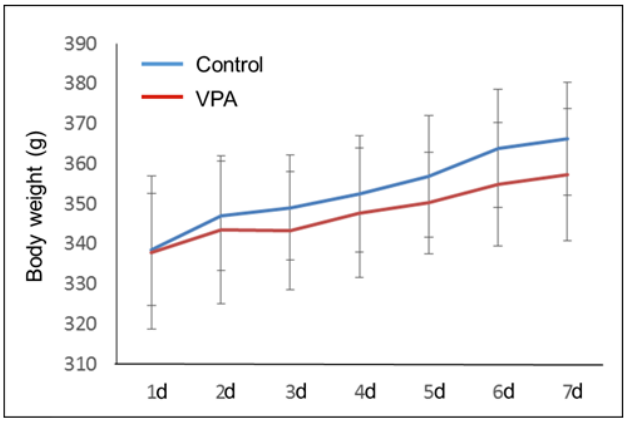

Figure 2: Body weights of control (n=27) and experimental groups (n=27) during the period of saline or valproic acid (VPA) injection.

Micro-CT images and bone analysis

Micro-CT images showed greater amounts of newly formed bone in the defect cavities of experimental animals when compared to controls at 7 (control, n=6, and VPA, n=6) and 14 (control, n=6 and VPA, n=6) days after defect formation (Figure 3a-3h).

After 21 days (control, n=6, and VPA, n=6), defects are prepared to be completely healed in the experimental group (Figure 3i-3l).

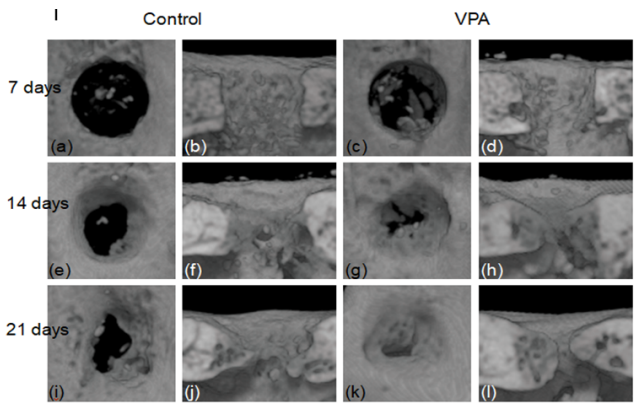

Figure 3: Micro-CT images of maxillary bone defects on days 7 (a-d), 14 (e-h), and 21 (i-l). Horizontal (a, c, e, g, i, k) and sagittal views (b, d, f, h, j, l).

Quantitative analysis of newly formed bone showed a gradual increase in BV/TV in both groups from day 7 to 21. However, the experimental group showed significantly higher BV/TV than controls at 14 (control, 40.358 ± 7.7132 vs 50.342 ± 5.4293 $p<0.05$) and 21 days (control, 53.635 ± 1.6555 vs VPA, 67.182 ± 3.385 $p<0.05$) (Figure 4a). Tb.Th also increased gradually in both groups; however, the experimental group showed higher Tb.Th than the control group at 14 (control, 166.0 ± 20.625 vs VPA, 207.50 ± 17.139 $p<0.05$) and 21 (control, 216.64 ± 3.9387 vs VPA, 250.39 ± 12.688 $p<0.05$) days after defect preparation (Figure 4b). A gradual decrease in Tb.Sp was observed in both the experimental and control groups from days 7 to 21. Nevertheless, at 14 (control, 211.82 ± 7.0889 vs VPA, 159.2 ± 0.6276 $p<0.05$) and 21 (control, 215.48 ± 21.448 vs VPA, 113.29 ± 8.6634 $p<0.05$) days after defect preparation, the experimental group showed significantly less Tb.Sp than the control group (Figure 4c).

Serum ALP activity

Serum ALP activity was increased gradually in both groups after bone cavity preparation. However, VPA treated animals showed significantly higher ALP activities at 7 (control, n=6 and VPA, n=6) (control, 0.3603 ± 0.005 vs VPA, 1.966 ± 0.001 $p<0.05$), 14 (control, n=6 and VPA, n=6) (control, 1.7506 ± 0.001 vs VPA, 2.3746 ± 0.001 $p<0.05$), and 21 (control, n=6 and VPA, n=6) (control, 1.5880 ± 0.001 vs VPA, 4.1570 ± 0.001 $p<0.05$) days when compared with the control group (Figure 4d).

Observations

Three days after cavity preparation

The control group showed numerous red blood cells and inflammatory cells in the defected area (Figure 5a and 5b). On the other hand, the defect area in the experimental group was mainly occupied by inflammatory cells (Figure 5c and 5d). In the center of the defect, cell debris and bone fragments were observed in both groups. Preexisting bone facing cutting edge contained empty osteocytic lacunae (Figure 5b and 5d).

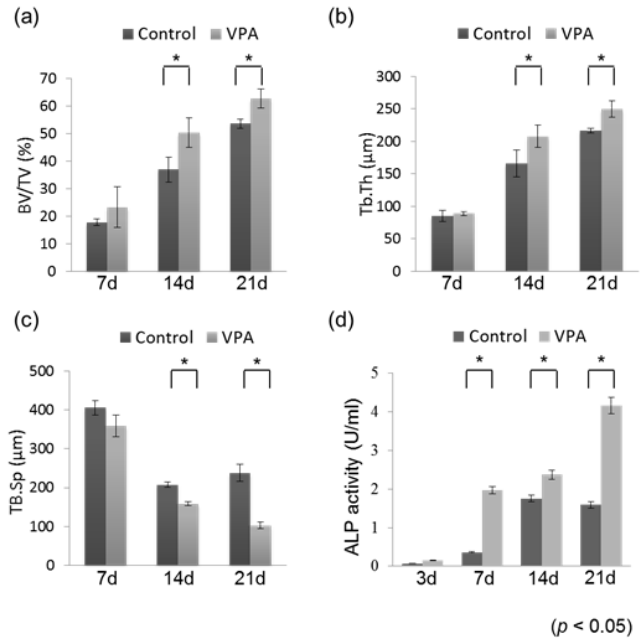

Figure 4: Micro-CT analysis of newly formed bone (a, b, c) and serum ALP activity measurement (d). Bone volume fraction (BV/TV) (a), trabecular thickness (Tb.Th) (b), and trabecular separation (Tb.Sp) (c). Serum alkaline phosphatase (ALP) activity was assessed on days 3 (n=6), 7 (n=6), 14 (n=6), and 21 (n=6) (d) after defect preparation.

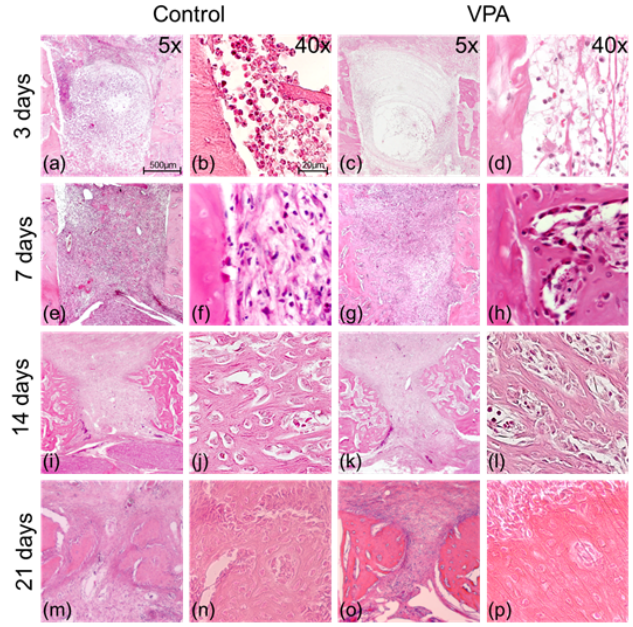

Figure 5: Histological specimens on days 3 (a-d), 7 (e-h), 14 (i-l), and 21 (m-p). Lower magnification (x5) images show the healing process for each bone cavity (a, c, e, g, i, k, m, and o). High magnification (x40) images (b, d, f, h, j, l, n, and p) show cell contributions for new bone formation. Hematoxylin-Eosin (H-E) stain.

Seven days after cavity preparation

At 7 days after defect preparation, no new bone formation was observed in the control group (Figure 5e and 5f); on the other hand, new bone formation was observed in the experimental group at the periphery of the defect. Newly formed bone was continuous to the preexisting bone (Figure 5g). Cuboidal or conical shaped osteoblast-like cells were arranged uniformly on the surface of the newly formed bone (Figure 5h). Bone with empty osteocytic lacunae remained present at the lateral wall of the cavity in both groups. The volume of cellular elements was observed to be equally distributed in all defect areas. No marked changes in histological features of the preexisting bone were observed at this stage (Figure 5f and 5h).

Fourteen days after cavity preparation

New bone formation was observed in both the control and experimental groups; however, the amount of newly formed bone was greater in experimental animals than in the control group (Figure 5i-5l). Newly formed bone was extended from the surface of the parent bone into the bone defect in both groups. Osteoblast-like cells, which had appeared cuboidal in shape at day 7 after defect formation, had become flattened. Several wide bone marrow areas surrounded by osteoblasts were observed in the newly formed bone in both groups (Figure 5j and 5l).

Twenty-one days after cavity preparation

The amount of newly formed bone was greater in the experimental group than in the control group (Figure 5m-5p). In the newly formed bone, an irregular woven structure was observed in the control group (Figure 5n and 5p). On the other hand, a lamella-like structure was observed in the experimental group (Figure 5n and 5p). Bone marrow areas in newly formed bone became narrower than after 14 days in both groups.

Microarray analysis

To understand VPA accelerate bone cavity healing effect, we performed microarray analysis to the bone marrow osteogenic cells in the experimental group and control group. In the VPA injected bone marrow (n=3), 12 genes exhibited more than a 2-fold increase compare to the control bone marrow (n=3), which include Collagen triple helix repeat containing 1 (Cthrc1), Carboxypeptidase A3 (Cpa3), colony stimulating factor 2 receptor-beta (Csf2rb), cholesterol 25-hydroxylase (Ch25h), tryptase alpha/beta 1 (Tpsab1), transforming growth factor, beta induced (Tgfbi), RT class II locus Da (RT-1Da), integrin, alpha 10 (Itga10), C1q and tumor necrosis factor related protein 3 (C1qtnf3), potassium channel subfamily T member 1 (Kctnt1), GATA binding protein 2 (Gata2) and sex comb on mid-leg-like 4 (Scml4). 14 genes showed more than 2-fold decrease including integrin, alpha 1 (Itga1), lectin-mannose-binding 2-like (Lman2l), SH3 domain containing ring finger 1 (Sh3rf1), thrombomodulin (Thbd), insulin-like growth factor binding protein 3 (Igfbp3), potassium voltage-gated channel, Shal-related subfamily 3 (Kcnd3), NAD kinase domain containing 1

(Nadkd1), secreted frizzled-related protein 2 (Sfrp2), a disintegrin-like and metalloprotease 9 (Adamts9), ribosomal protein L6 (Rpl6), gremlin 2 (Grem2), nephroblastoma overexpressed gene (Nov), FERM domain containing 6 (Frmd6) and Cell death-inducing DFFA-like effector (Cidec) (Table 1).

Upregulated genes	
Cpa3	Carboxypeptidase A3, mast cell
Csf2rb	colony stimulating factor 2 receptor-beta
Cthrc 1	collagen triple helix repeat containing 1
Ch25h	cholesterol 25-hydroxylase
Tpsab1	tryptase alpha/beta 1
Tgfbi	transforming growth factor, beta-induced
RT1-Da	RT class II locus Da
Itga 10	integrin, alpha 10
C1qtnf3	C1q and tumor necrosis factor related protein 3
Kctnt 1	potassium channel, subfamily T, member 1
Gata2	GATA binding protein 2
Scml4	sex comb on midleg-like 4
Downregulated genes	
Itga1	integrin, alpha 1
Lman2l	lectin,mannose-binding 2-like
Sh3rf1	SH3 domain containing ring finger 1
Thbd	thrombomodulin
Igfbp3	insulin-like growth factor binding protein
Kcnd3	potassium voltage-gated channel, Shal-related subfamily
Nadkd1	NAD kinase domain containing 1
Sfrp2	secreted frizzled-related protein 2
Adamts 9	a disintegrin-like and metalloprotease 9
Rpl6	ribosomal protein L6
Grem2	gremlin 2
Nov	nephroblastoma overexpressed gene
Frmd6	FERM domain containing 6
Cidec	Cell death-inducing DFFA-like effector

Table 1: Genes differentially expressed in a femoral bone marrow-derived cell by VPA injection.

Discussion and Conclusion

Clinical outcome of dental implants strongly depends upon the regeneration of bone tissue, which should be qualitatively and quantitatively adequate, and rapidly produced. As several studies have shown that HDACi have successfully enhanced osteogenic differentiation in different cells and/or cell lines through transcriptional regulation [23,24,31], in our current strategy, we attempted to regenerate bone tissue through systemic administration of VPA in an animal model. As an anti-epilepsy drug for human, VPA administrated 25~30 mg/kg/day and its half-life was known for 9-16 hours. In our study, we started the experiment with VPA dose from 10 to 500 mg /kg/day. However, there no big changes were found in the experimental animals. It might be because the half-life of VPA in the rat were shorter than human. Therefore, we used a higher dose for the experiment. Moreover, with consideration of VPA half-life in rat body, we administrated VPA twice a day. From the previous report, one of the possible effects of VPA treatment is body weight change, which in turn is thought to influence bone health [32]. However, weight effects might not completely explain the VPA-treatment on bone healing observed in this study. Because none of the VPA-treated animals actually lost weight during the injection period and among individual VPA-treated animals in this concentration (VPA at a dose of 300 mg/kg twice daily). However, a higher dose (350, 400, 450 and 500 mg/kg twice daily) VPA injection made weight loss to the experimental animals (data not shown). In this study, there were no correlations between total body mass measurements and the newly formed bone measurements. Micro-CT images showed greater amounts of new bone formation in VPA-treated animals than the control group. Higher BV/TV and Tb.Th suggested that osteoblastic activity was elevated in the experimental group. Increased distance between individual trabeculae (Tb.Sp) in the control group suggested a looser trabecular structure than in the experimental group. VPA is widely used as an antiepileptic drug. Interestingly, patients with epilepsy show an increased fracture risk [33]. In addition, long-term oral VPA administration demonstrated a negative effect on bone growth and density [34,35]. Thus, it has been extensively studied how antiepileptic drugs affect bone turnover; however, no correlations between valproate medication and loss in Bone Mineral Density (BMD) has been observed [36,37]. The changes in BMD do not appear to be caused by VPA, but rather are attributed to decreased physical activity levels, vitamin D deficiency, and secondary hyperparathyroidism [24]. In addition, it is likely that the relatively high dose and long-term therapy with VPA may be responsible for these adverse effects [23,35,38]. Numerous studies have reported that HDACi stimulates *in vitro* osteogenesis by increasing the expression of osteogenic genes, such as osteopontin, ALP, collagen-1α, osteocalcin, and bone sialoprotein [23,34,39]. To our knowledge, no *in vivo* experiments to date have been conducted for assessing bone regeneration with systemic injection of VPA. Results from serum ALP measurement indicated that VPA might have stimulated osteoblast bone formation ability through acceleration of osteoblast differentiation or increased number of osteoblasts and/or activity. As a result, bone defect healing was accelerated. No ectopic bone formation was observed in the experimental group. Thus, new bone formation only occurred at the healing site of the bone cavity. Results from histological analysis also showed marked bone defect healing with systemic injection of VPA in the experimental group. Earlier bone formation at 7 days after cavity preparation and greater amounts of newly formed bone at the later stages of the healing period in the experimental group than in the control group indicated that osteoblast activity and/or number increased in the rat body under VPA systemic injection. Although the underlying mechanisms of how VPA accelerated new bone formation were unclear in this study, HDACi demonstrated the osteoblastic differentiation of Mesenchymal Stem Cells (MSCs) through Runx2 activation [23,39-41]. From the histological analysis and serum ALP level, there was the possibility that VPA administration could upregulate bone turn-over and accelerate bone cavity healing. In this

study, we have not done bone turn over analysis using Fluorescent calcium chelating agent as a biomarker. It would indicate us the further mechanisms of cavity healing acceleration. Furthermore, several *in vivo* studies stated that bone marrow stem cells or MSCs migrated out of the marrow space and differentiated into osteoblasts at the site of fracture repair or bone formation [42-44] or ectopic bone formation [45]. We can, therefore, speculate that, in our study, VPA injection activated bone marrow stromal cells that contain bone marrow stem cells and osteoblast precursors. These cells move to the defect healing site through the bloodstream and differentiate into osteoblasts. VPA may also stimulate local precursors around the healing site. As a result, osteoblast number and/or activity increased and bone formation was accelerated. Further investigation regarding the healing mechanism remains necessary to confirm this speculation.

Because deacetylation of core histones by HDACs is associated with a 'closed' chromatin conformation and repression of transcription, inhibition of HDACs is thought to lead to activation of transcription. In fact, HDACi is known to affect gene expression in various cells [46-48]. Multiple HDACs are expressed by osteoblasts. They may play specific roles in regulating osteoblast differentiation. Some HDACs (HDAC 3 and HDAC 6) interact with Runx2 and repress Runx-2-dependent transcriptional activity. VPA with other HDACi has been shown to be able to block these HDACs and increased transcriptional activity of the osteoblast differentiation marker genes through Runx2 [19,23,24]. From microarray analysis, VPA injected bone marrow osteogenic cells showed a significant increase for gene expression in 12 genes. From these genes, there were no osteogenic differentiation marker genes but osteogenic related or bone metabolism related genes. For instance, Collagen triple helix repeat containing 1 (Cthrc1) which known as a coupling factor included in the upregulated genes group. Osteoclast secreted Cthrc1 promoted osteoblast bone formation [49]. Even though the maxilla cavity was far from femoral bone marrow, VPA i.p injection inducing Cthrc1 up-regulation might be contributing to defect healing. In addition, C1qtnf3 also known as Cor26, promoted cell calcification and involved in skeletal development [50,51]. GATA2 had differentiation ability for bone-marrow-derived mesenchymal stem cell [52]. Those genes might be affected by new bone formation through osteoblast activation. However, some upregulated genes also related to osteoclast activation. Oxysterol corded by Ch25h recruited osteoclast through EBI2 expression [53] and GATA2 also reported as an osteoclast development factor [54]. This osteoclast genesis and development related gene expressions might indicate the possibility that negative feedback of osteoblast activation or acceleration of bone metabolism. Fourteen genes showed down-regulation by VPA injection in microarray analysis. Among them, Gremlin [55], lectin [56], Nov (also known as CCN3) [57], SFRP2 [58] and IGFBP3 [59] were reported as a negative regulator for osteoblast. VPA injection might release repression of osteoblast activity by those 5 genes. Function and contribution for accelerations of bone defect healing by other genes were not clear. Because bone marrow-derived cells were heterogeneous and target cells for microarray were indefinite. Further investigation for those 26 altered genes would help to understand bone defect and fracture healing mechanisms. In this study, even though rapidly growing period, the bone defect model at 8 weeks old rats were used. Because bone formation could easily occur and be observed in comparison with adult rat defect healing models, ectopic bone formation models or extra bone formation models. We convinced that the model may facilitate a comparison of the effects of HDACi on bone formation. As VPA turned accelerated bone formation in the bone cavity, it could be interpreted that VPA is effective at improving bone formation in the case of bone augmentation. Of course, we could use this method to accelerate the osseointegration, which is the result of bone formation at the interface between bone and implant. In conclusion, this study clearly demonstrated that the systemic injection of VPA accelerated healing of the maxillary bone cavity. Therefore, the systemic administration of VPA is a potential treatment for bone regeneration or augmentation prior to or upon implant therapy.

Acknowledgment

This study was supported by a Grand-in-AID for Scientific Research (C) Grant number 25462988、26462915. The authors declare no potential conflicts of interest with respect to the authorship and/or publication of this article.

References

1. Becker W, Becker BE, Caffesse R (1994) A comparison of demineralized freeze-dried bone and autologous bone to induce bone formation in human extraction sockets. J Periodontol 65: 1128-1133.
2. Egusa H, Sonoyama W, Nishimura M, Atsuta I, Akiyama K (2012) Stem cells in dentistry-Part II: Clinical applications. J Prosthodont Res 56: 229-248.
3. Crespi R, Vinci R, Capparè P, Gherlone E, Romanos GE (2006) Calvarial versus iliac crest for autologous bone graft material for a sinus lift procedure: a histomorphometric study. Int J Oral Maxillofac Implants 22: 527-532.
4. Van Steenberghe D, Naert I, Bossuyt M, De Mars G, Calberson L, et al. (1997) The rehabilitation of the severely resorbed maxilla by simultaneous placement of autogenous bone grafts and implants: a 10-year evaluation. Clin Oral Investig 1: 102-108.
5. Haas R, Donath K, Fodinger M, Watzek G (1998) Bovine hydroxyapatite for maxillary sinus grafting: Comparative histomorphometric findings in sheep. Clin Oral Implants Res 9: 117-122.
6. Lee CY (2006) Immediate load protocol for anterior maxilla with cortical bone from mandibular ramus. Implant Dent 15: 153-159.
7. Babiker H, Ding M, Sandri M, Tampieri A, Overgaard S, et al. (2012) The effects of bone marrow aspirate, bone graft, and collagen composites on fixation of titanium implants. J Biomed Mater Res B Appl Biomater 100: 759-766.
8. Dahlin C, Simion M, Nanmark U, Sennerby L (1998) Histological morphology of the e- FTFE/tissue interface in humans subjected to guided bone regeneration in conjunction with oral implant treatment. Clin Oral Implants Res 9: 100-106.
9. Payer M, Lohberger B, Strunk D, Reich KM, Acham S, et al. (2014) Effects of directly autotransplanted tibial bone marrow aspirates on bone regeneration and osseointegration of dental implants. Clin Oral Implants Res 25: 468-474.
10. Schimming R, Schmelzeisen R (2004) Tissue-engineered bone for maxillary sinus augmentation. J Oral Maxillofac Surg 62: 724-729.
11. Ivanovski S (2009) Periodontal regeneration. Aust Dent J 54: S118-S128.
12. Sahrmann P, Attin T, Schmidlin PR (2011) Regenerative treatment of peri-implantitis Using bone substitutes and membrane: A systematic review. Clin Implant Dent Relat Res 13: 46-57.
13. Oreffo RO, Cooper C, Mason C, Clements M (2005) Mesenchymal stem cells. Stem Cell Rev 1: 169-178.
14. Lotem J, L Sachs (2006) Epigenetics and the plasticity of differentiation in normal and cancer stem cells. Oncogene 25: 7663-7672.
15. Alexanian AR (2007) Epigenetic modifiers promote efficient generation of neural-like cells from bone marrow-derived mesenchymal cells grown in neural environment. J Cell Biochem 100: 362-371.
16. Feinberg AP (2007) Phenotypic plasticity and the epigenetics of human disease. Nature 447: 433-440.

17. Delcuve GP, Rastegar M, Davie JR (2009) Epigenetic control. J Cell Physiol 219: 243-250.
18. Lehrmann H, Pritchard LL, Harel-Bellan A (2002) Histone acetyltransferases and deacetylases in the control of cell proliferation and differentiation. Adv Cancer Res 86: 41-65.
19. Westendorf JJ, Zaidi SK, Cascino JE, Kahler R, van Wijnen AJ, et al. (2002) Runx2 (Cbfa1, AML-3) interacts with histone deacetylase 6 and represses the p21CIP1/WAF1 promoter. Mol Cell Biol 22: 7982-7992.
20. Schroeder TM, Kahler RA, Li X, Westendorf JJ (2004) Histone deacetylase 3 interacts with runx2 to repress the osteocalcin promoter and regulate osteoblast differentiation. J Biol Chem 279: 41998-42007.
21. Lee HW, Suh JH, Kim AY, Lee YS, Park SY, et al. (2006) Histone deacetylase 1-mediated histone modification regulates osteoblast differentiation. Mol Endocrinol 20: 2432-2443.
22. Jensen ED, Schroeder TM, Bailey J, Gopalakrishnan R, Westendorf JJ (2008) Histone deacetylase 7 associates with Runx2 and represses its activity during osteoblast maturation in a deacetylation-independent manner. J Bone Miner Res 23: 361-372.
23. Cho HH, Park HT, Kim YJ, Bae YC, Suh KT, et al. (2005) Induction of osteogenic differentiation of human mesenchymal stem cells by histone deacetylase inhibitors. J Cell Biochem 96: 533-542.
24. Schroeder TM, Westendorf JJ (2005) Histone deacetylase inhibitors promote osteoblast maturation. J Bone Miner Res 20: 2254-2263.
25. Jeon EJ, Lee KY, Choi NS, Lee MH, Kim HN, et al. (2006) Bone morphogenetic protein-2 stimulates Runx2 acetylation. J Biol Chem 281: 16502-16511.
26. Gottlicher M, Minucci S, Zhu P, Kramer OH, Schimpf A, et al. (2001) Valproic acid defines a novel class of HDAC inhibitors inducing differentiation of transformed cells. EMBO J 20: 6969-6978.
27. Phiel CJ, Zhang F, Huang EY, Guenther MG, Lazar MA, et al. (2001) Histone deacetylase is a direct target of valproic acid, a potent anticonvulsant, mood stabilizer, and teratogen. J Biol Chem 276: 36734-36741.
28. Duncan HF, Smith AJ, Fleming GJ, Cooper PR (2012) Histone deacetylase inhibitors induced differentiation and accelerated mineralization of pulp-derived cells. J Endod 38: 339-345.
29. Feng HL, Leng Y, Ma CH, Zhang J, Ren M, et al. (2008) Combined lithium and valproate treatment delays disease onset, reduces neurological deficits and prolongs survival in an amyotrophic lateral sclerosis mouse model. Neuroscience 155: 567-572.
30. Ayalogu OE, Igboh NM, Dede EB (2001) Biochemical changes in the serum and liver of albino rats exposed to petroleum samples (gasoline, kerosene, and crude Petroleum). Journal of Applied Sciences and Environmental Management 5.
31. Maroni P, Brini AT, Arrigoni E, Girolamo L, Niada S, et al. (2012) Chemical and genetic blockade of HDACs enhances osteogenic differentiation of human adipose tissue-derived stem cells by oppositely affecting osteogenic and adipogenic transcription factors. Biochem Biophys Res Commun 428: 271-277.
32. Senn SM, Kantor S, Poulton IJ, Morris MJ, Sims NA, et al. (2010) Adverse effects of valproate on bone: Defining a model to investigate the pathophysiology. Epilepsia 51: 984-993.
33. Ecevit Ç, Aydoğan A, Kavakli T, Altinöz S (2004) Effect of carbamazepine and valproate on bone mineral density. J Pediatr 31: 279-282.
34. Souverein PC, Webb DJ, Weil JG, Van Staa TP, Egberts ACG (2006) Use of antiepileptic drugs and risk of fractures Case-control study among patients with epilepsy. Neurology 66: 1318-1324.
35. Nissen-Meyer LSH, Svalheim S, Taubøll E, Reppe S, Lekva T, et al. (2007) Levetiracetam, phenytoin, and valproate act differently on rat bone mass, structure, and metabolism. Epilepsia 48: 1850-1860.
36. Triantafyllou N, Lambrinoudaki I, Armeni E, Evangelopoulos EM, Boufidou F, et al. (2010) Effect of long-term valproate monotherapy on bone mineral density in adults with epilepsy. J Neurol Sci 290: 131-134.
37. Aksoy A, Sönmez FM, Deger O, Hosver I, Karagüzel G (2011) The effects of antiepileptic drugs on the relationships between leptin levels and bone turnover in prepubertal children with epilepsy. J Pediatr Endocrinol Metab 24: 703-708.
38. Sato Y, Kondo I, Ishida S, Motooka H, Takayama K, et al. (2001) Decreased bone mass and increased bone turnover with valproate therapy in adults with epilepsy. Neurology 57: 445-449.
39. Boer JD, Licht R, Bongers M, Klundert TV, Arends R, et al. (2006) Inhibition of histone acetylation as a tool in bone tissue engineering. Tissue Eng 12: 2927-2937.
40. Huangfu D, Maehr R, Guo W, Eijkelenboom A, Snitow M, et al. (2008) Induction of pluripotent stem cells by defined factors is greatly improved by small-molecule compounds. Nature biotechnology 26: 795-797.
41. Shakibaei M, Shayan P, Busch F, Aldinger C, Buhrmann C, et al. (2012) Resveratrol mediated modulation of Sirt-1/Runx2 promotes osteogenic differentiation of mesenchymal stem cells: potential role of Runx2 deacetylation. PLoS One 7: e35712.
42. Devine MJ, Mierisch CM, Jang E, Anderson PC, Balian G (2002) Transplanted bone marrow cells localize to fracture callus in a mouse model. J Orthop Res 20: 1232-1239.
43. Taguchi K, Ogawa R, Migita M, Hanawa H, Ito H, et al. (2005) The role of bone marrow-derived cells in bone fracture repair in a green fluorescent protein chimeric mouse model. Biochem Biophys Res Commun 331: 31-36.
44. Kaku M, Akiba Y, Akiyama K, Akita D, Nishimura M (2015) Cell-based bone regeneration for alveolar ridge augmentation-Cell source, endogenous cell recruitment and immunomodulatory function. J Prosthodont Res 59: 96-112.
45. Otsuru S, Tamai K, Yamazaki T, Yoshikawa H, Kaneda Y (2007) Bone marrow-derived osteoblast progenitor cells in circulating blood contribute to ectopic bone formation in mice. Biochem Biophys Res Commun 354: 453-458.
46. Glaser KB, Staver MJ, Waring JF, Stender J, Ulrich RG, et al. (2003) Gene expression profiling of multiple histone deacetylase (HDAC) inhibitors: defining a common gene set produced by HDAC inhibition in T24 and MDA carcinoma cell lines. Mol Cancer Ther 2: 151-163.
47. L Tou, Liu Q, Shivdasani RA (2004) Shivdasani, Regulation of mammalian epithelial differentiation and intestine development by class I histone deacetylases. Mol Cell Biol 24: 3132-3139.
48. Yokota T, Matsuzaki Y, Miyazawa K, Zindy F, Roussel MF, et al. (2004) Histone deacetylase inhibitors activate INK4d gene through Sp1 site in its promoter. Oncogene 23: 5340-5349.
49. Takeshita S, Fumoto T, Matsuoka K, Park K, Aburatani H, et al. (2013) Osteoclast-secreted CTHRC1 in the coupling of bone resorption to formation. J Clin Invest 123: 3914-3924.
50. Maeda T, Abe M, Kurisu K, Jikko A, Furukawa S (2001) Molecular cloning and characterization of a novel gene, CORS26, encoding a putative secretory protein and its possible involvement in skeletal development. J Biol Chem 276: 3628-3634.
51. Zhou Y, Wang J, Feng H, Wang C, Li L, et al. (2014) Overexpression of C1q/tumor necrosis factor-related protein-3 promotes phosphate-induced vascular smooth muscle cell calcification both in vivo and in vitro. Arterioscler Thromb Vasc Biol 34: 1002-1010.
52. Kamata M, Okitsu Y, Fujiwara T, Kanehira M, Nakajima S, et al. (2014) GATA2 regulates differentiation of bone marrow-derived mesenchymal stem cells. Haematologica 99: 1686-1696.
53. Nevius E (2013) EBI2 guides osteoclast precursors to bone niches and regulates osteoclastogenesis and bone mass homeostasis.(P5099). J Immun 190 (Meeting Abstracts 1): 129.14.
54. Yamane T (2000) Sequential requirements for SCL/tal-1, GATA-2, macrophage colony-stimulating factor, and osteoclast differentiation factor/osteoprotegerin ligand in osteoclast development. Exp Hematol 28: 833-840.
55. Pereira RC (2000) Bone morphogenetic proteins induce gremlin, a protein that limits their activity in osteoblasts. Endocrinology 141: 4558-4563.

56. Nakamura A, Ly C, Cipetić M, Sims NA, Vieusseux J, et al. (2007) Osteoclast inhibitory lectin (OCIL) inhibits osteoblast differentiation and function in vitro. Bone 40: 305-315.

57. Matsushita Y, Sakamoto K, Tamamura Y, Shibata Y, Minamizato T, et al. (2013) CCN3 protein participates in bone regeneration as an inhibitory factor. J Biol Chem 288: 19973-19985.

58. Oshima T (2005) Myeloma cells suppress bone formation by secreting a soluble Wnt inhibitor, sFRP-2. Blood 106: 3160-3165.

59. Li J, Jin D, Fu S, Mei G, Zhou J, et al. (2013) Insulin-like growth factor binding protein-3 modulates osteoblast differentiation via interaction with vitamin D receptor. Biochem Biophys Res Commun 436: 632-637.